Characteristics of HfO_2 thin films deposited by plasma-enhanced atomic layer deposition using O_2 plasma and N_2O plasma

Seokhoon Kim, Jinwoo Kim, Jihoon Choi, et al.

Citation: Journal of Vacuum Science & Technology B: Microelectronics and Nanometer Structures Processing, Measurement, and Phenomena **24**, 1088 (2006); doi: 10.1116/1.2188405

View online: https://doi.org/10.1116/1.2188405

View Table of Contents: https://avs.scitation.org/toc/jvn/24/3

Published by the American Institute of Physics

Characteristics of HfO_2 thin films deposited by plasma-enhanced atomic layer deposition using O_2 plasma and N_2O plasma

Seokhoon Kim, Jinwoo Kim, Jihoon Choi, Hyunseok Kang, and Hyeongtag Jeon[a)]
Division of Materials Science and Engineering, Hanyang University, Seoul 133-791, Korea

Choelhwyi Bae
System LSI Division, Samsung Electronics Co., Ltd., Yongin Gyeonggi-do 449-711, Korea

(Received 9 December 2005; accepted 24 February 2006; published 21 April 2006)

The characteristics of HfO_2 dielectrics deposited by the plasma-enhanced atomic layer deposition (PEALD) method using O_2 and N_2O plasmas were investigated. The deposited HfO_2 films had a randomly oriented polycrystalline phase while the interfacial layers of the films were amorphous. During the PEALD process with N_2O plasma, nitrogen was mainly incorporated into the interfacial region between the HfO_2 film and the Si substrate. The nitrogen content of 2–3 at. % in the interface was analyzed by Auger electron spectroscopy. The incorporated nitrogen at the interface effectively suppressed residual oxygen diffusion during subsequent annealing at 800 °C in a N_2 atmosphere. A thicker interfacial layer was observed in the as-deposited and annealed HfO_2 film with O_2 plasma than with N_2O plasma. For HfO_2 films prepared with the N_2O plasma, where equivalent oxide thickness (EOT) increased from 1.43 to 1.56 nm after annealing, the leakage current densities, measured at a gate bias voltage of $|V_G - V_{FB}| = 2$, increased from 3.5×10^{-8} to 4.8×10^{-8} A/cm^2. For HfO_2 films prepared with the O_2 plasma, where EOT increased from 1.60 to 2.01 nm after annealing, the leakage current densities decreased from 1.1×10^{-6} to 1.3×10^{-7} A/cm^2. The film with O_2 plasma had a higher amount of negative fixed oxide charges than the film with N_2O plasma. N_2O plasma improved the leakage current properties by allowing nitrogen incorporation at the interfacial region and less crystallization of HfO_2 film.
 [DOI: 10.1116/1.2188405]

I. INTRODUCTION

Conventional SiO_2 gate dielectrics suffer from leakage and reliability deficiencies as the SiO_2 thickness in the metal-oxide-semiconductor field effect transistors (MOSFETs) decreases below 2.0 nm.[1] One solution to effectively reduce the equivalent oxide thickness (EOT) without increasing the leakage current is to use high dielectric constant (high-*k*) materials.[2] This application of high-*k* gate dielectrics to replace SiO_2 is now actively investigated. Metal-organic chemical vapor deposition (MOCVD) and atomic layer deposition (ALD) have been widely studied in an effort to grow high-*k* gate dielectrics.[3,4] These deposition methods exhibit the good uniformity and damage-free film characteristics compared to physical vapor deposition (PVD) methods. However, contaminations such as hydrogen, halogens, and organic species can deteriorate the electrical properties of films grown at low temperatures by MOCVD and ALD methods.[5,6] Therefore, the plasma application in the ALD process is one way to solve these problems because plasma effects increase reactivity, reduce impurities, and densify the film.[7] Among the high dielectric constant materials, HfO_2, Al_2O_3, and ZrO_2 have been widely studied as next-generation semiconductor devices that solve the problems of excessive high leakage current.[8,9] HfO_2 is considered to be one of the most promising materials among these high dielectric materials. HfO_2 exhibits desirable properties such as high dielectric constant (κ=25–30), high density (~9.65 g/cm^3), large band gap (5.68 eV), and thermal stability in contact with silicon.[10] Unfortunately, HfO_2 crystallizes at temperatures less than 500 °C.[11] Grain boundaries found in crystallized HfO_2 can be used as diffusion paths for oxygen or dopants through the oxide layer, causing a threshold voltage instability, and the generation of defects.[12] The formation of an uncontrolled interfacial layer at the HfO_2/Si interface also limits further scaling down of EOT of HfO_2 gate dielectric. HfO_2 films have also shown a poor thermal stability after subsequent thermal processes, which results in an increase of leakage current. However, several research groups have recently reported that the incorporation of nitrogen into high-*k* materials can improve the material's thermal stability.[13,14] Incorporation of nitrogen atoms into the HfO_2 films during deposition would prevent crystallization of the HfO_2 film and interfacial reactions between the HfO_2 and Si after annealing.

In this study, we utilized the plasma-enhanced atomic layer deposition (PEALD) system and focused on the effect of the incorporated nitrogen in HfO_2 films during PEALD process when using N_2O plasma. The characteristics of the HfO_2 films deposited by PEALD using N_2O plasma were then compared to that of the films deposited using O_2 plasma.

[a)]Author to whom correspondence should be addressed; electronic mail: hjeon@hanyang.ac.kr

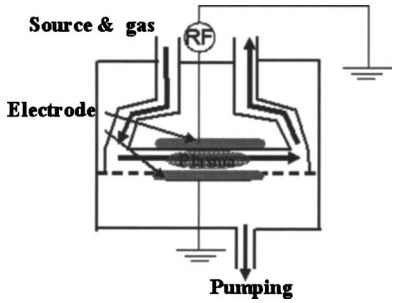

FIG. 1. Schematic of the PEALD system.

II. EXPERIMENT

The HfO_2 films were deposited on *p*-type Si (100) wafers at 340 °C by the PEALD method using O_2 or N_2O plasma with tetrakis-diethyl-amino-hafnium $[Hf(N(C_2H_5)_2)_4]$, as the Hf precursor. Si wafers were cleaned with a piranha solution ($H_2O_2:H_2SO_4=1:4$) for 10 min to remove organic contaminants, washed in de-ionized (DI) water, and then dipped for 2 min in a dilute HF solution (HF:DI water=1:100) to remove native oxides. The clean wafers were then rinsed in DI water again, dried in nitrogen, and loaded into the ALD chamber. Figure 1 shows the schematic drawing of PEALD system. The Hf precursor, $Hf(N(C_2H_5)_2)_4$, was vaporized at 90 °C and introduced into the reaction chamber by using a bubbler with Ar as the carrier gas. The O_2 plasma and N_2O plasma were used as the oxygen reactants. The basic one cycle consisted of supplying the Hf precursor and then exposing the plasma. Ar purge gas was introduced to promote the complete separation of the Hf precursor and plasma. All gas flows were automatically controlled by using a solenoid valve. For the HfO_2 film, the sequential processing time for the $Hf(N(C_2H_5)_2)_4$, Ar purge, plasma, and Ar purge were 5, 7, 5, and 7 s, respectively. The plasma source used was a radio-frequency (rf) source of 13.56 MHz and a fixed power of 100 W. The process pressure was maintained at 0.5 torr by automatic control with a throttle valve. The metal-oxide-semiconductor (MOS) capacitors were fabricated with an ~5 nm thick HfO_2 film and a Pt electrode with a thickness of ~100 nm. For postdeposition annealing (PDA), the films were rapidly annealed at 800 and 1000 °C for 1 min in a N_2 atmosphere. A postmetallization annealing (PMA) was also carried out in a 97% N_2/3% H_2 mixed atmosphere at 450 °C for 30 min. The physical thickness of the HfO_2 films and interfacial layers were analyzed by cross-sectional transmission electron microscopy (XTEM). The chemical states and bonding structure of the HfO_2 films were investigated using x-ray photoelectron spectroscopy (XPS). Auger electron spectroscopy (AES) was utilized to analyze variations in chemical composition, the content of the impurities, and the amount of incorporated nitrogen. The electrical properties and reliability characteristics including EOT, hysteresis, capacitance, and leakage current were measured using a Keithley 590 *C-V* analyzer and an HP 4155A semiconductor parameter analyzer.

III. RESULTS AND DISCUSSION

Figure 2 shows the AES depth profiles of as-grown HfO_2 films using (a) O_2 plasma and (b) N_2O plasma at a deposition temperature of 340 °C. The AES depth profile of both samples shows the stoichiometric composition of the HfO_2 films. The carbon contents in the HfO_2 films deposited with O_2 plasma and N_2O plasma were approximately 1–2 at. %. As shown in Fig. 2(b), the nitrogen content at the interfacial region of the HfO_2 films deposited with the N_2O plasma was approximately 2–3 at. %, while nitrogen atoms were not detected in the HfO_2 film deposited with the O_2 plasma, as seen in Fig. 2(a). The nitrogen atoms were incorporated not in HfO_2 film but at the interfacial region of the film during the PEALD process using the N_2O plasma. Lucovsky reported that nitrogen is incorporated at the $Si-SiO_2$ interface and not in the bulk of the thin SiO_2 in the remote-plasma-assisted oxidation (RPAO) process using N_2O.[15] The AES result of Fig. 2(b) shows that the nitrogen is incorporated at the $Si-HfO_2$ interface during HfO_2 deposition using N_2O plasma.

Figure 3 shows XPS spectra of the Hf 4*f* for the as-deposited and annealed ~5 nm thick HfO_2 films with O_2

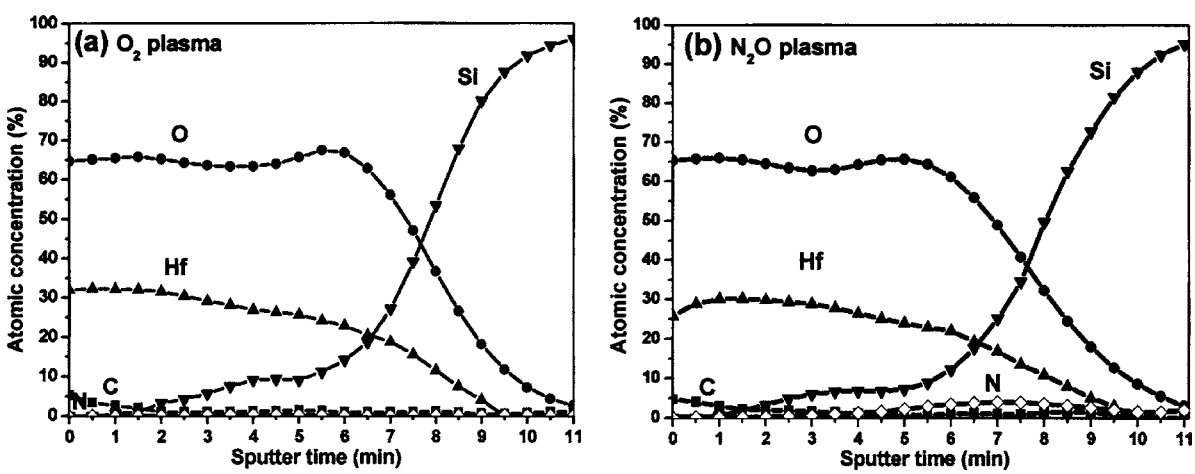

FIG. 2. AES depth profiles of as-deposited HfO_2 films using (a) O_2 plasma and (b) N_2O plasma at a deposition temperature of 340 °C.

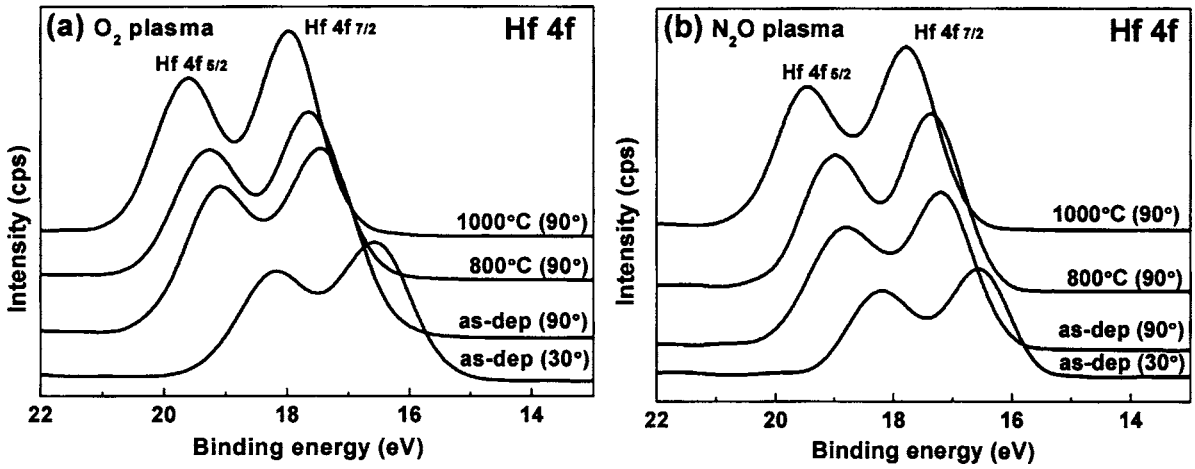

FIG. 3. XPS spectra of the Hf 4*f* for the ~5 nm thick HfO_2 films after a PDA at temperatures of 800 and 1000 °C for 1 min in a N_2 atmosphere: (a) HfO_2 films deposited with O_2 plasma and (b) HfO_2 films deposited with N_2O plasma. The as-deposited films were measured at take-off angles of 30° and 90°.

plasma and N_2O plasma. The PDA was performed at temperatures of 800 and 1000 °C for 1 min in a N_2 atmosphere. The as-deposited films were measured at take-off angles of 30° and 90°. At take-off angle of 30°, the signal from the HfO_2 film becomes greatly enhanced relative to that from the interfacial region between HfO_2 and Si. At take-off angle of 90°, the signal at the interface of HfO_2 and Si becomes enhanced. We calibrated all the peaks with the C 1*s* peak position at the 285 eV. Wilk *et al.* reported that the Hf $4f_{7/2}$ peak of Hf silicate is ~1.0 eV higher than that of the HfO_2, which is located at ~16.5–17 eV.[16] As shown in the Hf $4f_{7/2}$ peaks of Fig. 3, as-deposited HfO_2 films with O_2 or N_2O plasma exhibit a binding energy of ~16.5 eV at take-off angle of 30°. At take-off angle of 90°, Hf $4f_{7/2}$ peaks of as-deposited HfO_2 films with O_2 and N_2O plasmas are located at ~17.4 and ~17.0 eV, respectively. Therefore, the films are considered to consist of HfO_2 and Hf silicate, where the Hf silicate is in the interfacial layer. The nitrogen incorporated in the interface by the N_2O plasma in Fig. 2(b) may also contribute to the peak shift toward a lower binding energy than Hf $4f_{7/2}$ peaks position of HfO_2 film deposited with O_2 plasma in Fig. 3. When the annealing temperatures of HfO_2 samples were increased, the Hf $4f_{7/2}$ peak at take-off angle of 90° shifted from ~17.4 to ~18.0 eV for O_2 plasma and from ~17.1 to ~17.8 eV for N_2O plasma. The Hf $4f_{7/2}$ peak for O_2 plasma shifted to a higher binding energy, as compared with N_2O plasma. This indicates that the nitrogen incorporated into the interface of HfO_2 film by the N_2O plasma effectively suppressed the growth of the Hf silicate layer.

Figures 4(a) and 4(b) show the XPS spectra of the Si 2*p* of the ~5 nm thick HfO_2 films deposited with O_2 plasma and N_2O plasma, respectively, after the PDA at 800 and 1000 °C for 1 min in a N_2 atmosphere. The HfO_2 films were measured at take-off angle of 90° to observe the growth of interfacial layer with annealing temperature. The Si 2*p* peak at ~99 eV originated from a Si substrate. The binding energies observed between ~102 and ~103.3 eV corresponded to the interfacial layer. As the annealing temperatures increased, the intensities of the XPS peaks corresponding to

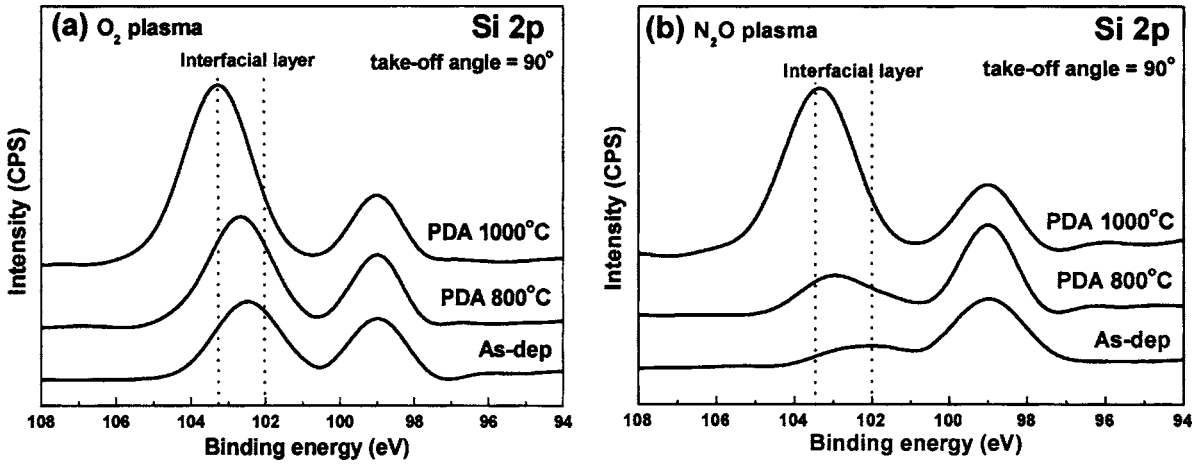

FIG. 4. XPS spectra of Si 2*p* for the ~5 nm thick HfO_2 films after a PDA at the temperatures of 800 and 1000 °C for 1 min in a N_2 atmosphere: (a) HfO_2 films deposited with O_2 plasma and (b) HfO_2 films deposited with N_2O plasma. The films were measured at take-off angle of 90°.

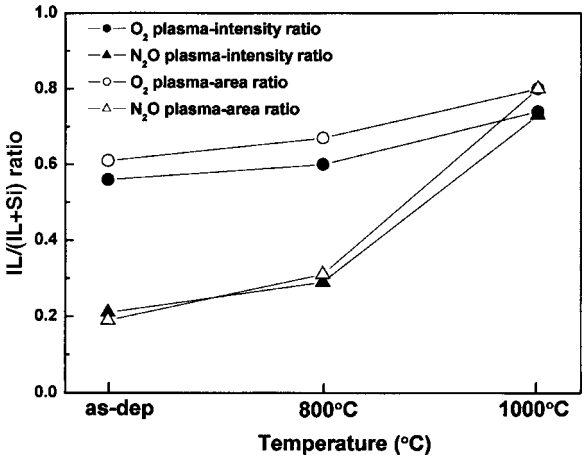

FIG. 5. Intensity and area ratios of Si 2*p* peaks measured at take-off angle of 90° with varying PDA temperatures. The intensity and area ratios, IL/(IL+Si), were calculated by fitting with a Gaussian function.

the interfacial layer increased, which corresponded to a growth of the interfacial layer. However, the interfacial layers of HfO_2 films with the N_2O plasma were thinner than those with the O_2 plasma up to a temperature of 800 °C. This indicates that the incorporated N atoms into the interfacial region by the N_2O plasma suppressed the growth of the interfacial layer.

Figure 5 shows the intensity and area ratio of Si 2*p* peaks measured at take-off angles of 90° varying with PDA temperatures. The intensity and area ratio of IL/(IL+Si) were calculated by fitting with a Gaussian function. The IL and Si represent the interfacial layer and silicon substrate, respectively. As the annealing temperature increased, the intensity and area ratio of IL/(IL+Si) increased. The intensity and area ratio of IL/(IL+Si) for N_2O plasma was lower than that for O_2 plasma up to a temperature of 800 °C, while the two were almost identical at 1000 °C after a sharp increase from 800 to 1000 °C. This shows that the interfacial layer formed by N_2O plasma is thinner than that formed by O_2 plasma up to temperatures of 800 °C. Therefore, the nitrogen incorporated into the interfacial layer acts as a reaction-diffusion barrier during the PEALD process.

Four images of Fig. 6 show cross-sectional TEM of approximately 5.5 nm HfO_2 deposited films. Figure 6(a) is an as-deposited sample with O_2 plasma and Fig. 6(b) is an annealed sample at 800 °C for 1 min. Figure 6(c) is an as-deposited sample with N_2O plasma and Fig. 6(d) is an annealed sample at 800 °C for 1 min. As shown in Fig. 6, the as-deposited and the annealed HfO_2 films exhibited a randomly oriented crystalline structure and their interfacial layers had an amorphous structure. We think that the metastable species in the plasma released their energy through collisions, resulting in the observed crystallization.[17] Therefore, the crystallization of the HfO_2 film grown by the PEALD method was considered to be caused by the metastable species in plasma which enhanced the reaction. The ions in the plasma physically attacked the film, and radicals chemically reacted with ligands of the $Hf(N(C_2H_5)_2)_4$ precursor during the PEALD process. The degree of crystallization of the HfO_2 film with O_2 plasma in Figs. 6(a) and 6(b) is larger compared to that with N_2O plasma in Figs. 6(c) and 6(d). The interfacial layers of HfO_2 film with O_2 plasma were thicker than those with the N_2O plasma, which agrees well with the XPS results in Fig. 5. The interfacial layer thickness of the HfO_2 film deposited using O_2 plasma increased from 2.6 to 3.0 nm, while those using N_2O plasma remained at a constant thickness of ~2.0 nm after PDA at 800 °C for 1 min. The thin interfacial layers in Figs. 6(c) and 6(d) are due to the incorporated nitrogen atoms in the interfacial region by the N_2O plasma. Therefore, nitrogen atoms incorporated in the interfacial region from the N_2O plasma, effectively suppressing the diffusion of residual oxygen and/or silicon into the film during deposition or annealing process and contributing to the suppression of the interfacial layer growth.

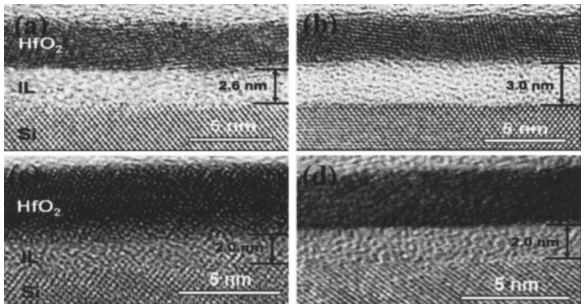

FIG. 6. Cross-sectional TEM images of approximately 5.5 nm HfO_2 deposited films. (a) is an as-deposited sample with O_2 plasma and (b) is an annealed sample at 800 °C for 1 min. (c) is an as-deposited sample with N_2O plasma and (d) is an annealed sample at 800 °C for 1 min.

Figure 7 shows the capacitance-voltage (*C-V*) curves of the HfO_2 films grown with (a) O_2 plasma and (b) N_2O plasma after an annealing treatment at 800 °C for 1 min. The *C-V* was measured at a frequency of 100 kHz. The gate voltage was swept from accumulation to inversion and back. The *C-V* curves showed maximum accumulation at high negative bias voltages. The corresponding EOT values of the as-deposited HfO_2 films with O_2 plasma and N_2O plasma were approximately 1.60 and 1.43 nm, respectively, and those of the 800° C annealed films were 2.0 and 1.56 nm, respectively. The increase of EOT is related to the interfacial layer growth and the increase in the total film thickness after annealing. The capacitance of the as-deposited HfO_2 film in the accumulation region decreased after annealing. This resulted from the decrease in the series capacitance due to the interfacial layer growth. Therefore, from a variation of capacitances in accumulation region of the *C-V* curves in Fig. 7, the nitrogen-incorporated HfO_2 films with the N_2O plasma suppressed the growth of the interlayer more effectively than the film deposited by O_2 plasma. This was also confirmed by the thickness of the interfacial layer that was obtained from high-resolution TEM (HRTEM) in Fig. 6. The flatband voltage of the *C-V* curves was shifted toward positive bias during sweeping. Since the electrons injected under a positive bias are not ejected rapidly, they induce a negative charge at

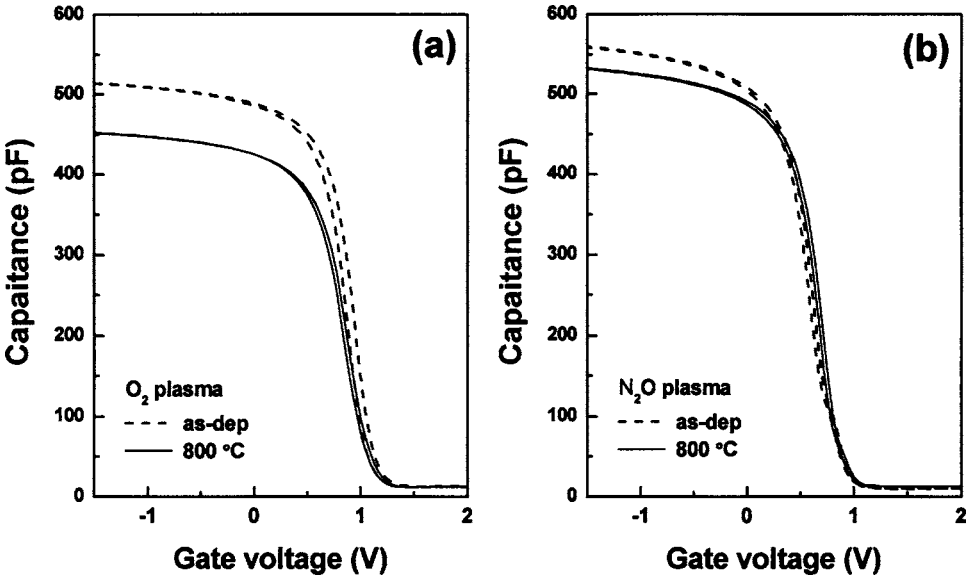

FIG. 7. Capacitance-voltage (C-V) curves of HfO_2 films grown using O_2 plasma and N_2O plasma after an annealing treatment at 800 °C for 1 min.

the interface of the HfO_2 films. The HfO_2 films showed a reversible hysteresis indicating that there is no significant effect from the deep traps in the bulk. For the HfO_2 film with O_2 plasma, the flatband voltage (V_{FB}) and effective fixed oxide charge density ($Q_{f,\mathrm{eff}}$) decreased from 1.23 to 1.18 and from -6.01×10^{12} to -4.84×10^{12} q/cm^2, respectively, as a result of the annealing process. For those with N_2O plasma, V_{FB} and $Q_{f,\mathrm{eff}}$ decreased from 0.91 to 0.89 and from -2.95×10^{12} to -2.57×10^{12} q/cm^2, respectively. Therefore, the film with O_2 plasma had a higher amount of negative fixed oxide charges than those with N_2O plasma.

Figure 8 shows the current-voltage (J-V) curves of the HfO_2 films grown by O_2 plasma and N_2O plasma after an annealing treatment at 800 °C for 1 min. The leakage current densities of the as-deposited and annealed HfO_2 films measured at a gate bias voltage of $|V_G-V_{FB}|=2$ were 1.1×10^{-6} and 1.3×10^{-7} $\mathrm{A/cm}^2$ in the case of the O_2 plasma and 3.5×10^{-8} and 4.8×10^{-8} $\mathrm{A/cm}^2$ in the case of the N_2O plasma, respectively. The reduction of leakage current density of the HfO_2 films deposited using O_2 plasma after annealing is believed to be due to changes in the growth of the amorphous interfacial layer and the film densification caused by postdeposition annealing. The nitrogen incorporation at the interfacial region and less crystallization due to the N_2O plasma resulted in an improvement of the leakage current properties. Table I summarizes the electrical characteristics of the HfO_2 films deposited by using PEALD.

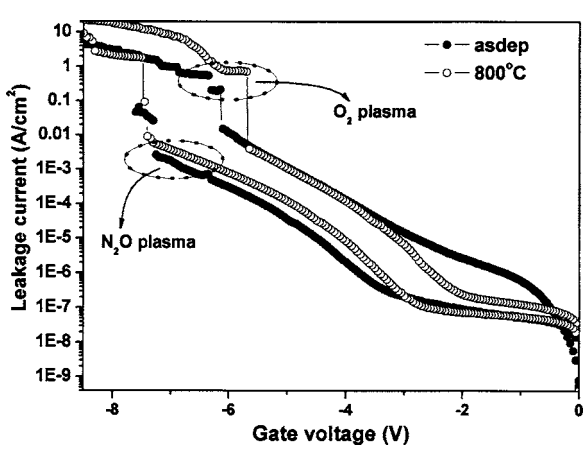

FIG. 8. Current-voltage (J-V) curves of HfO_2 films grown using O_2 plasma and N_2O plasma after an annealing treatment at 800 °C for 1 min.

IV. CONCLUSIONS

HfO_2 films were successfully deposited on Si substrates using $Hf(N(C_2H_5)_2)_4$ as a precursor with O_2 plasma and N_2O plasma. The nitrogen atoms were incorporated at the interfacial region of the HfO_2 film during the PEALD process using N_2O plasma. The interfacial layer of HfO_2 films with N_2O plasma was thinner than films with O_2 plasma up to a temperature of 800 °C. HfO_2/IL/Si structure deposited by N_2O plasma was shown to be more resistant to oxygen diffusion. The nitrogen atoms incorporated into the interface of the HfO_2 film by the N_2O plasma effectively suppressed the growth of the interfacial Hf silicate layer. The HfO_2 films deposited with the N_2O plasma also showed improved film quality with a relatively low EOT, low leakage current density, and low effective fixed oxide charge density compared

TABLE I. Summary of the electrical characteristics of HfO_2 films deposited by PEALD using O_2 plasma and N_2O plasma. LKG represents leakage current density measured at $|V_G-V_{FB}|=2$. V_{FB} and $Q_{f,\mathrm{eff}}$ represents flatband voltage and effective fixed oxide charge density, respectively.

Oxygen reactant	Annealing temperature (°C)	EOT (nm)	LKG ($\mathrm{A\,cm}^{-2}$)	V_{FB} (V)	$Q_{f,\mathrm{eff}}$ ($q\,\mathrm{cm}^{-2}$)
O_2 plasma	As deposited	1.60	1.1×10^{-6}	1.23	-6.01×10^{12}
	800	2.01	1.3×10^{-7}	1.18	-4.84×10^{12}
N_2O plasma	As deposited	1.43	3.5×10^{-8}	0.91	-2.95×10^{12}
	800	1.56	4.8×10^{-8}	0.89	-2.57×10^{12}

to films deposited with the O_2 plasma. Therefore, the N_2O plasma process can improve the physical and electrical properties of HfO_2 film.

ACKNOWLEDGMENTS

This work was supported by the National Program for Tera-level Nanodevices of the Ministry of Science and Technology as one of the 21th century Frontier Programs.

[1]W.-K. Kim, S.-W. Rhee, N.-I. Lee, J.-H. Lee, and H.-K. Kang, J. Vac. Sci. Technol. A **22**, 1285 (2004).
[2]K. Yamamoto, M. Asai, S. Horii, H. Miya, and M. Niwa, J. Vac. Sci. Technol. A **21**, 1033 (2003).
[3]K. P. Bastos *et al.*, Appl. Phys. Lett. **81**, 1669 (2002).
[4]M. M. Frank, S. Sayan, S. Dörmann, T. J. Emge, L. S. Wielunski, E. Garfunkel, and Y. J. Chabal, Mater. Sci. Eng., B **109**, 6 (2004).
[5]O. Sneh, R. B. Clark-Phelps, A. R. Londergan, J. Winkler, and T. E. Seidel, Thin Solid Films **402**, 248 (2002).
[6]K. Kukli, M. Ritala, J. Aarik, T. Unstare, and M. Leskel, J. Appl. Phys. **92**, 1833 (2002).
[7]Y. Kim, J. Koo, J. Han, S. Choi, H. Jeon, and C. Park, J. Appl. Phys. **92**, 5443 (2002).
[8]S. Gopalan, K. Onishi, R. Nieh, C. S. Kang, R. Choi, H.-J. Cho, S. Krishnan, and J. C. Lee, Appl. Phys. Lett. **80**, 4416 (2002).
[9]J. Lee, J. Koo, H. S. Sim, and H. Jeon, J. Korean Phys. Soc. **44**, 915 (2004).
[10]M. Balog, M. Schieber, M. Michiman, and S. Patai, Thin Solid Films **41**, 247 (1977).
[11]G. D. Wilk, R. M. Wallace, and J. M. Anthony, J. Appl. Phys. **89**, 5243 (2001).
[12]S. H. Bae, C. H. Lee, R. Clark, and D. L. Kwong, IEEE Electron Device Lett. **24**, 556 (2003).
[13]C. H. Choi, S. J. Rhee, T. S. Joen, N. Lu, J. H. Sim, R. Clark, M. Niwa, and D. L. Kwong, Tech. Dig. - Int. Electron Devices Meet. 857 (2002).
[14]W. J. Zhu, T. Tamagawa, M. Gibson, T. Furukawa, and T. P. Ma, IEEE Electron Device Lett. **23**, 649 (2002).
[15]G. Lucovsky, IBM J. Res. Dev. **43**, 308 (1999).
[16]G. D. Wilk, R. M. Wallace, and J. M. Anthony, J. Appl. Phys. **87**, 484 (2000).
[17]J. Kim, S. Kim, H. Jeon, M.-H. Cho, K.-B. Chung, and C. Bae, Appl. Phys. Lett. **87**, 053108 (2005).